THE JOURNAL OF BIOLOGICAL CHEMISTRY
Vol. 275, No. 32, Issue of August 11, pp. 24313–24320, 2000

Printed in U.S.A.

Differential Protein Phosphorylation in 3T3-L1 Adipocytes in Response to Insulin *Versus* Platelet-derived Growth Factor

NO EVIDENCE FOR A PHOSPHATIDYLINOSITIDE 3-KINASE-INDEPENDENT PATHWAY IN INSULIN SIGNALING*

Received for publication, March 6, 2000, and in revised form, April 17, 2000)
Published, JBC Papers in Press, May 8, 2000, DOI 10.1074/jbc.M001823200

Michelle M. Hill‡§, Lisa M. Connolly¶, Richard J. Simpson¶, and David E. James‡‖

From the ‡Centre for Molecular and Cellular Biology and the Department of Physiology and Pharmacology, University of Queensland, St. Lucia, Queensland 4072 Australia and the ¶Joint Protein Structure Laboratory, Ludwig Institute of Cancer Research and the Walter and Eliza Hall Institute, Parkville, Victoria 3050, Australia

Insulin regulates glucose metabolism in adipocytes via a phosphatidylinositide 3-kinase (PI3K)-dependent pathway that appears to involve protein phosphorylation. However, the generation of phosphoinositides is not sufficient for insulin action, and it has been suggested that insulin regulation of glucose metabolism may involve both PI3K-dependent and -independent pathways, the latter being insulin specific. To test this hypothesis, we have designed a phosphoprotein screen to study insulin-specific phosphoproteins that may be either downstream or in parallel to PI3K. Nineteen insulin-regulated phosphospots were detected in the cytosol and high speed pellet fractions, only six of which were significantly regulated by platelet-derived growth factor. Importantly, almost all (92%) of the insulin-specific phosphoproteins identified using this approach were sensitive to the PI3K inhibitor wortmannin. Thus, we obtained no evidence for an insulin-specific, PI3K-independent signaling pathway. A large proportion (62%) of the insulin-specific phosphoproteins were enriched in the same high speed pellet fraction to which PI3K was recruited in response to insulin. Thus, our data suggest that insulin specifically stimulates the phosphorylation of a novel subset of downstream targets and this may in part be because of the unique localization of PI3K in response to insulin in adipocytes.

Insulin stimulates glucose uptake into muscle and fat cells mainly through the translocation of glucose transporter 4 (GLUT4)[1] from an intracellular location to the cell surface (1). This mechanism is crucial for the maintenance of glucose homeostasis. An impairment in insulin-stimulated glucose uptake is a major factor leading to the development of non insulin-dependent diabetes mellitus (2). Insulin binding to its cell surface receptor activates the intrinsic tyrosine kinase activity of the insulin receptor and stimulates tyrosine phosphorylation of insulin receptor substrate proteins. Tyrosine-phosphorylated IRS proteins in turn recruit Src homology 2 domain-containing signaling proteins. Two main pathways have been identified downstream of IRS proteins, the mitogen-activated protein (MAP) kinase pathway and the phosphatidylinositide 3-kinase (PI3K) pathway. The PI3K pathway, through protein kinase B (PKB), has been shown to be necessary for insulin-stimulated glucose transport through various experimental approaches. First, two structurally unrelated inhibitors of PI3K, wortmannin and LY294002, potently inhibit insulin-stimulated glucose transport in adipocytes (3, 4). Second, dominant negative mutants of the p110 catalytic subunit (5), the p85 regulatory subunit of PI3K (6), or PKB (7) inhibit insulin-stimulated glucose transport in adipocytes. In addition, microinjection of a PKB substrate peptide or an antibody to PKB inhibit insulin-stimulated GLUT4 translocation in 3T3-L1 adipocytes (8). Finally, constitutively active PI3K (9) or PKB (10) trigger GLUT4 translocation independently of insulin when expressed in adipocytes.

Whereas evidence supports a role for the PI3K/PKB pathway in insulin-stimulated GLUT4 translocation in adipocytes, other growth factors also activate PI3K without stimulating GLUT4 translocation, raising the question of signaling specificity (reviewed in Ref. 11). In particular, platelet-derived growth factor (PDGF) stimulates PI3K activity to the same extent as insulin in adipocytes but has relatively little effect on glucose transport (12–17). Several hypotheses have been advanced to account for this controversy. One possibility is that these different growth factors may activate unique PI3K isoforms with different substrate specificities. It has also been proposed that PI3K may be activated in different locations in response to insulin *versus* PDGF (13, 14, 18). Several studies have shown that in response to PDGF, most of the increase in PI3K occurs in the plasma membrane (PM) fraction. In contrast, following insulin stimulation, there is a large increase in PI3K activity in a high speed pellet (HSP) fraction. This fraction also contains the major insulin regulatable IRS proteins (IRS1 and IRS2) found in insulin-sensitive cells (13, 14, 18). One potential consequence of this discrete localization is that PI3K may access different

* This work was supported by grants from the National Health and Medical Research Council of Australia and the Juvenile Diabetes Foundation International. The Centre for Molecular and Cellular Biology is a Special Research Center of the Australian Research Council. The costs of publication of this article were defrayed in part by the payment of page charges. This article must therefore be hereby marked "*advertisement*" in accordance with 18 U.S.C. Section 1734 solely to indicate this fact.

§ Present address: Friedrich Miescher Institute, Postfach 2543, CH-4002, Basel, Switzerland.

‖ National Health and Medical Research Council Principal Research Fellow. To whom correspondence should be addressed**:** Centre for Molecular and Cellular Biology, University of Queensland, St. Lucia, Queensland, Australia, 4072. Tel.: 61 7 3365 4986; Fax: 61 7 3365 4430; E-mail: D.James@cmcb.uq.edu.au.

[1] The abbreviations used are: GLUT4, glucose transporter 4; IRS, insulin receptor substrate; MAP kinase, mitogen-activated protein kinase; PI3K, phosphatidylinositide 3-kinase; PKB, protein kinase B; PDGF, platelet-derived growth factor; PM, plasma membrane; HSP, high speed pellet; PIP_3, phosphatidylinositol 3,4,5-trisphosphate; 2-DE, two-dimensional gel electrophoresis; HPLC, high pressure liquid chromatography; MS, mass spectrometry; EF, elongation factor; ACL, ATP-citrate lyase.

downstream targets. Alternatively, the activation of glucose metabolism by insulin may require activation of the PI3K pathway as well as an additional, insulin-specific pathway. The finding that membrane-permeant analogs of phosphatidylinositol 3,4,5-trisphosphate (PIP_3) do not activate glucose uptake when added to adipocytes suggests that activation of PI3K may not be sufficient to stimulate GLUT4 translocation, leading to the hypothesis that a PI3K-independent pathway is also required (19).

Each of these models predicts that insulin must trigger a unique signal transduction pathway, that either lies downstream or in parallel to PI3K. Despite this prediction, little progress has been made in elucidating such a novel pathway. Thus, in the present study, we designed a subtraction assay based on protein phosphorylation to select for molecules that may be regulated in an insulin-specific manner. A differential screening procedure using two-dimensional gels was employed to select for phosphoproteins that are specifically regulated by insulin, and not PDGF, in a wortmannin-sensitive manner. Insulin stimulated the phosphorylation of 18 phosphoprotein spots. Only six of these proteins were phosphorylated by PDGF in a manner that was quantitatively comparable to insulin. In addition, insulin specifically stimulated the dephosphorylation of one row of phosphospots. Interestingly, insulin-specific phosphoproteins preferentially localized to the HSP fraction, further confirming the presence of insulin-specific targets in this fraction. With the possible exception of one phosphospot, all of the insulin-specific phosphoproteins were wortmannin-sensitive. Hence, based on these studies we have found no evidence of an insulin-activated PI3K-independent pathway involving protein phosphorylation in 3T3-L1 adipocytes. These results suggest that insulin activates an unique, PI3K-dependent pathway, which regulates metabolism in adipocytes.

EXPERIMENTAL PROCEDURES

Antibodies—Antibodies against mitogen-activated protein kinase were described previously (20). Antibodies specific for mitogen-activated protein kinase phosphorylated at Thr^{202} and Tyr^{204} were from New England Biolabs (Beverly, MA). Rabbit antibodies against PKBβ were generously provided by Dr. M. Birnbaum (Philadelphia, PA).

Generation of Phosphorylation Maps—For radiolabeling, 3T3-L1 adipocytes were incubated in a buffer containing 12.5 mM HEPES, pH 7.4, 120 mM NaCl, 6 mM KCl, 1.2 mM Mg_2SO_4, 1 mM $CaCl_2$, 0.2 mM $NaPO_4$, 2% (w/v) bovine serum albumin, and 0.5 mCi/ml $^{32}P_i$ (ICN) for 2 h at 37 °C. Labeled cells were then incubated with: 1) insulin (1 μM) for 15 min, 2) wortmannin (100 nM) for 25 min and wortmannin plus insulin (1 μM) for a further 15 min, 3) PDGF $\beta\beta$ (50 ng/ml, Life Technologies, Inc.) for 15 min, or 4) no additions. After treatment, cells were washed in ice-cold HES buffer (20 mM HEPES, pH 7.4, 1 mM EDTA, 250 mM sucrose) and then homogenized in HES buffer supplemented with protease inhibitors (10 μg/ml aprotinin, 10 μg/ml leupeptin, and 1 mM phenylmethylsulfonyl fluoride) and phosphatase inhibitors (1 mM sodium orthovanadate, 1 mM sodium pyrophosphate, 1 mM ammonium molybdate and 10 mM sodium fluoride) by ten passes through a 22 gauge needle. Subcellular fractionation by differential centrifugation was performed as described previously (21).

The PM and HSP pellets were directly solubilized in 2-DE sample buffer (9 M urea, 40 mM Tris, 4.4% CHAPS, 84 mM dithiothreitol, 1% Pharmalyte, 1 mM phenylmethylsulfonyl fluoride and phosphatase inhibitors as above). The cytosol fraction was precipitated with 4 sample volumes of ice-cold acetone for 10 min and then centrifuged for 5 min at 10,000 $\times$ *g* at room temperature. The resulting protein pellets were solubilized in 2-DE sample buffer. Protein concentration was determined by the method of Bradford (Bio-Rad), and 150 μg of each fraction was loaded onto the gel. 2-DE, silver staining, and autoradiography were performed as described (21).

Analysis of Phosphorylation Maps—Autoradiographs were digitized using a densitometer (Molecular Analyst, Bio-Rad), and analyzed using Melanie II 2D analysis software (Bio-Rad). Detailed analysis was performed on HSP and cytosol fractions obtained from basal, insulin-, PDGF- and wortmannin-plus-insulin-treated cells from five separate experiments. Gel spots were detected by the software and manually checked. Spot intensity was measured as volumes (integration of optical density over area) and then normalized to the overall volume for each gel to account for gel-to-gel variations within each experiment. Gels were aligned using dominant phosphoproteins present in all gels as landmarks. Gel spots were matched across the four treatment groups for each experiment by the software and then manually checked. The normalized values for matched spots from basal *versus* insulin-treated cells were compared for significant changes that were consistent between five experiments using paired *t* tests. Values for corresponding spots were expressed as a percentage of the insulin-stimulated value, as shown in Tables I and II. The molecular mass and pI of phosphoprotein spots were calculated by the analysis software using the following landmark proteins (mass/pI): actin, (42 kDa/5.29), α-enolase (47 kDa/6.24), ATP-citrate lyase (ACL, 121 kDa/6.96), bovine serum albumin (bovine serum albumin, 66 kDa), cytosolic malate dehydrogenase (36 kDa/6.16), elongation factor 2 (95 kDa/6.41), and vimentin (54 kDa/5.06). Landmark proteins were identified by immunoblotting or sequencing.

Immunoblot Analysis of Two-dimensional Gels—Proteins were transferred to polyvinylidene difluoride membranes (Immobilon-P from Millipore) according to the method of Towbin *et al.* (22). After blocking nonspecific binding sites with 5% skim milk powder in Tris-buffered saline/Tween (TBST, 50 mM Tris, pH 7.5, 150 mM NaCl, 0.1% Tween-20), membranes were incubated with the relevant primary antibodies diluted in blocking buffer for 2 h at room temperature or overnight at 4 °C. After washing in TBST, membranes were incubated with horseradish peroxidase-conjugated secondary antibody (Amersham Pharmacia Biotech) diluted 1/10,000 in TBST for 1 h at room temperature. After washing in TBST, antibody bound was visualized using Supersignal chemiluminescence substrate (Pierce) and Fuji film.

Preparative 2-DE and In-gel Tryptic Digestion—For sequence analysis of phosphoprotein spots, a combined cytosol + HSP fraction (6 mg) from insulin-stimulated cells was subjected to SDS-polyacrylamide gel electrophoresis. Regions between 35 and 55 kDa, and from 100 to 200 kDa were excised and electroeluted using a Bio-Rad electroeluter. The eluate was concentrated in a speed-vac. SDS was removed by methanol-chloroform precipitation (23), and the protein precipitate was resolubilized in 2-DE sample buffer containing 7 M urea and 2 M thiourea. Samples prepared from one preparative SDS-polyacrylamide gel electrophoresis gel were combined with an aliquot of ^{32}P-labeled cytosol + HSP fraction (150 μg) prepared from insulin-stimulated cells, and loaded onto a two-dimensional gel. Preparative two-dimensional gels were stained with Coomassie, dried, and subjected to autoradiography to identify phosphoproteins of interest. As most phosphoprotein spots were not stained by Coomassie, corresponding spots were excised from multiple preparative two-dimensional gels and re-electrophoresed into one band as described previously (24). Coomassie-stained bands were excised and subjected to in-gel tryptic digestion (25).

Liquid Chromatography/Electrospray-Ion Trap Mass Spectrometry—An electrospray ion trap mass spectrometer (LCQ Finnigan MAT, San Jose, CA) coupled on-line with a capillary HPLC (Hewlett-Packard Model 1090A modified for capillary chromatography, as described in Ref. 26) was used for peptide sequencing. A 60-min linear gradient (flow rate 1.7 μl/min) was used from 0–100% solvent B, where solvent A was 0.1% v/v aqueous trifluoroacetic acid and solvent B was 0.1% aqueous trifluoroacetic acid in 60% acetonitrile. The electrospray parameters were as follows: spray voltage, 4.5 kV; sheath gas and auxiliary gas flow rates, 5 and 30 (arbitrary value), respectively; capillary temperature, 150 °C; capillary voltage, 20 V; and tube lens offset, 16 V. The sheath liquid used was 2-methoxyethanol (99.9% HPLC grade) delivered at a flow rate of 3 μl/min. The electron multiplier was set to -860 V, and the trap was allowed a maximum injection time of up to 200 ms. After acquiring one scan in MS, the most intense ion in that spectrum above a threshold of 1×10^5 was isolated for subsequent zoom scan and then collision-induced dissociation in the following scans. The dissociation energy was set to 55%.

Protein/Peptide Identification—The sequences of individual peptides were identified using the SEQUEST algorithm, incorporated into the Finnigan-MAT BIOWORKS software to correlate the uninterpreted collision-induced dissociation spectra with amino acid sequences in the OWL protein data base (27).

RESULTS

In the present study we have focused on protein phosphorylation as an assay for insulin signal transduction and action for several reasons. First, insulin is known to regulate a number of downstream actions via protein phosphorylation, including the

synthesis of lipid, glycogen, and protein. Second, a number of reagents that modulate protein phosphorylation including phosphatase inhibitors like okadaic acid have profound effects on insulin action (28). Finally, it is relatively simple using metabolic labeling to conduct a random large scale analysis of changes in protein phosphorylation in response to certain treatments. To increase the sensitivity of detection, analysis was performed on subcellular fractions rather than whole cell lysates, a technique first applied to adipocytes by Avruch *et al.* (29, 30). In these early studies, resolution of ^{32}P-labeled phosphoproteins by SDS-polyacrylamide gel electrophoresis revealed only one insulin-stimulated phosphoprotein of 123 kDa, which likely corresponds to ATP-citrate lyase (30). In the current study, we have utilized 2-DE to achieve higher resolution of ^{32}P-labeled phosphoproteins present in subcellular fractions of adipocytes. The use of 2-DE to resolve ^{32}P-labeled phosphoproteins has been previously reported (31, 32), albeit not in conjunction with subcellular fractionation. By combining radiolabeling with subcellular fractionation and 2-DE, we hoped to attain the resolution required to study the phosphorylation of low abundance phosphoproteins.

Three subcellular fractions have been studied in detail as indicated below. The rationale for selecting these particular fractions is based on our previous observation that the PM fraction contains the insulin and PDGF receptors, whereas the HSP fraction is enriched in IRS1 (18). In response to PDGF, PI3K is mainly recruited to the PM fraction, whereas in response to insulin it is recruited to the HSP fraction. Therefore, these different fractions potentially represent discrete loci for the assembly of signaling complexes. We have also studied the cytosolic fraction because it is also known to contain many signaling molecules including MAP kinase and PKB.

Insulin-stimulated Protein Phosphorylation in the High Speed Pellet and Cytosol Fractions—Initially we studied the polypeptide composition of PM, HSP, and cytosol fractions isolated from adipocytes. Using 2-DE and silver staining we identified >200 individual silver-stained spots/fraction (21). Most of the proteins resolved by this technique were in the molecular mass range of 20–120 kDa consistent with previous studies using this approach (31). Hence, it is unlikely that proteins outside this range including IRS1 and IRS2 would have been resolved. The overall pattern of silver-stained spots was quite different between the three fractions studied, consistent with the fact that they comprise distinct intracellular components (21). We were unable to detect any effect of insulin on the polypeptide composition among these fractions. Between 50 and 300 distinct phosphoprotein spots were detected in the PM, HSP, and cytosol fractions, and the overall pattern of these spots was significantly different between the different fractions. In agreement with previous studies (29, 30, 32), the phosphorylation of the majority of these spots was unaffected by insulin treatment (Figs. 1 and 2). However, quantitative analysis of five separate experiments showed that insulin consistently and significantly increased the phosphorylation of at least 18 spots (Figs. 1 and 2).

To further ascertain that our phosphoprotein mapping technique accurately reflects cellular phosphorylation, we first examined a well characterized insulin target, MAP kinase. Using an antibody specific for both the p42 and p44 MAP kinase isoforms we first showed that these proteins were enriched in the cytosol fraction of 3T3-L1 adipocytes (data not shown). Analysis of the cytosol fraction by 2-DE followed by immunoblotting allowed resolution of several immunoreactive spots migrating at the appropriate mass and pI of p44 and p42 MAP kinase (Fig. 3*A*). Following insulin stimulation, there was a leftward shift toward acidic pI for both p42 and p44 MAP

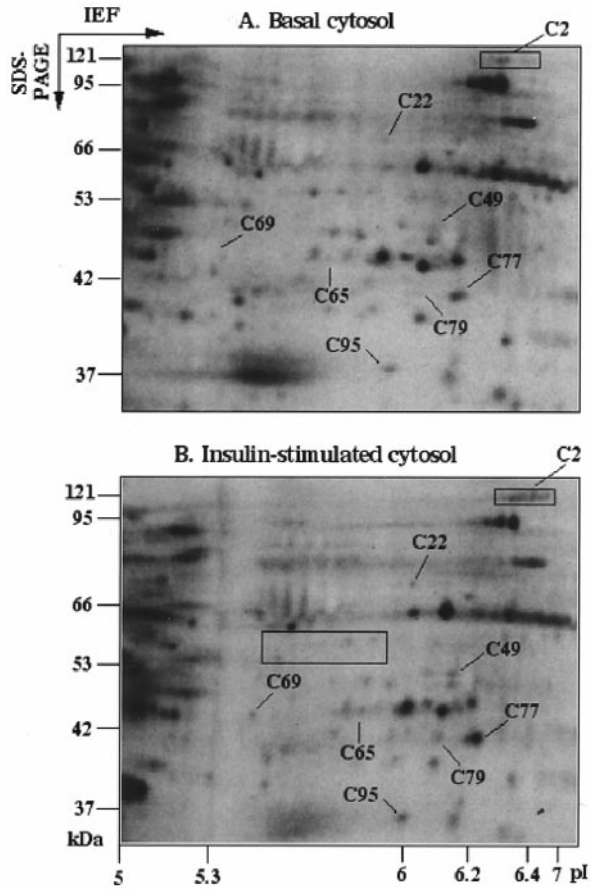

FIG. 1. **Phosphorylation maps of the cytosol fraction.** 3T3-L1 adipocytes were labeled with ^{32}P and incubated in the absence (*A*) or presence (*B*) of insulin for 15 min. Cells were homogenized and fractionated to generate a cytosol fraction, and this was subjected to 2-DE and autoradiography. Five separate experiments were analyzed quantitatively for insulin-regulated phosphoprotein spots. These are marked with spot numbers preceded by C for cytosol, and the results are summarized in Table I. *IEF*, isoelectric focusing.

kinase (Fig. 3*B*), and these spots could now also be detected using a phospho-MAP kinase antibody (Fig. 3*D*). Furthermore, ^{32}P-labeled spots were detected at the same position as the pI-shifted MAP kinase spots, but only in the insulin-stimulated cytosol fraction (C65, C79, Fig. 1). These results demonstrate that our technique is sensitive enough to detect changes in the phosphorylation of low abundance signaling proteins.

Similar studies to those described above were performed to determine if our screen could detect another major downstream target of insulin, PKB. PKB phosphorylation is induced by insulin in a PI3K-dependent manner (33). We have recently reported that PKBβ is the main isoform expressed in 3T3-L1 adipocytes, and it is enriched in the cytosol (8). To better resolve proteins in the molecular mass and pI range of PKB (58 kDa/pI 5.9), it was necessary to perform our mapping studies in buffer containing reduced levels of bovine serum albumin. Under these conditions, a row of ^{32}P-labeled spots was observed in the region of the gel corresponding to the predicted position of PKB (Fig. 4*A*). Insulin increased the phosphorylation of five of these spots (compare Fig. 4, *A* and *B*). To determine if any of these spots corresponded to PKBβ, ^{32}P-labeled cytosol fractions from basal or insulin-treated cells were analyzed by 2-DE and immunoblotting with a PKBβ antibody (Fig. 4, *C* and *D*). In the basal state, the PKBβ antibody detected four distinct spots (spots 0–3, Fig. 4*C*). In agreement with previous results (8), spots 1 and 2 overlapped with ^{32}P-labeled spots, representing constitutively phosphorylated PKBβ (Fig. 4, *A* and *C*). Insulin

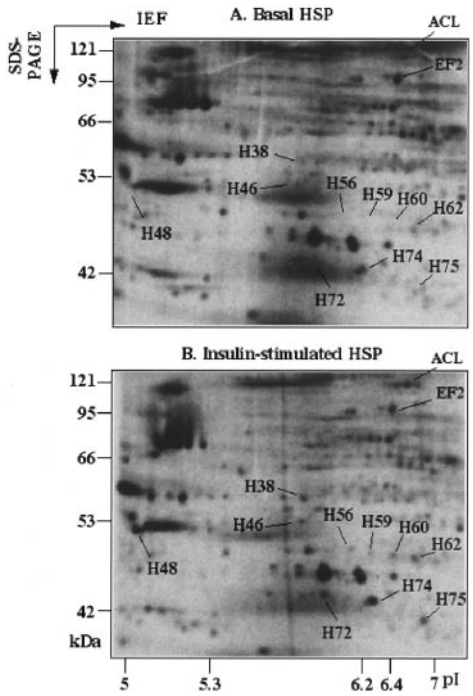

FIG. 2. **Phosphorylation maps of the HSP fraction.** 3T3-L1 adipocytes were labeled with ^{32}P and incubated in the absence (*A*) or presence (*B*) of insulin for 15 min. Cells were homogenized and fractionated to generate a HSP fraction, which was analyzed by 2-DE and autoradiography. Quantitative analysis was performed on five separate experiments for insulin-regulated phosphoprotein spots. These are marked with spot numbers preceded by H for HSP, and the results are summarized in Table II. *IEF*, isoelectric focusing.

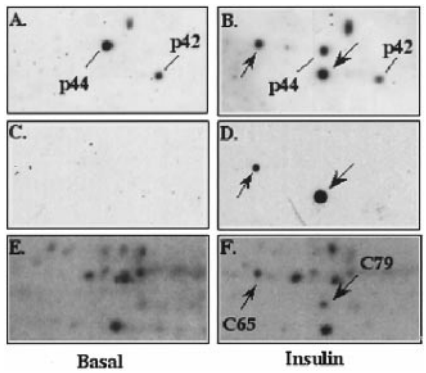

FIG. 3. **Identification of C65 and C79 as p44 and p42 MAP kinase.** 3T3-L1 adipocytes were ^{32}P-labeled and then incubated in the absence (*A*, *C*, and *E*) or presence of insulin (*B*, *D*, and *F*) for 15 min. Cytosol was isolated, subjected to 2-DE, and analyzed either by autoradiography (*E* and *F*) or by immunoblotting with (*A* and *B*) a pan-MAP kinase antibody or (*C* and *D*) a phospho-MAP kinase antibody.

stimulation increased the phosphorylation of spots 1–4 (Fig. 4, *A* and *B*), decreased the immunoreactivity of spots 0 and 1, and increased the immunoreactivity of spots 2–4 (Fig. 4, *C* and *D*). Other phosphospots detected in this region did not overlap with PKBβ-immunoreactive spots (indicated by *arrowheads* in Fig. 4, *A* and *B*) and likely represent other phosphoproteins of similar molecular mass and pI.

Effects of Insulin, PDGF, and Insulin Plus Wortmannin on Protein Phosphorylation—The screen that we have designed to identify a putative insulin-specific signaling pathway in adipocytes is based on the fact that adipocytes express receptors for PDGF, but PDGF does not activate glucose metabolism in these cells (13, 14, 18). Furthermore, the PI3K inhibitor wortmannin potently inhibits insulin regulation of metabolism. Thus, we

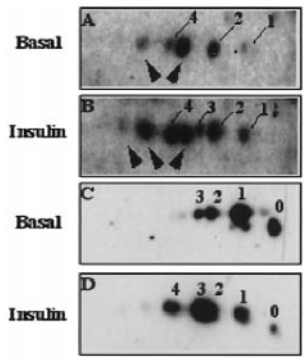

FIG. 4. **Insulin induces PKBβ phosphorylation.** 3T3-L1 adipocytes were ^{32}P-labeled in Krebs-Ringer phosphate buffer containing 0.1% bovine serum albumin, and then left untreated (*A* and *C*) or stimulated with insulin (*B* and *D*). Cytosol fractions (150 μg) were analyzed by 2-DE and autoradiography (*A* and *B*) or immunoblotting with a PKBβ antibody (*C* and *D*). The corresponding region in cytosol maps is indicated by the *box* in Fig. 1*B*.

reasoned that this technique should enable us to resolve an insulin-specific, PDGF-insensitive pathway by comparing the effects of these different compounds on protein phosphorylation. A series of experiments were performed to compare the protein phosphorylation pattern between insulin, PDGF, and insulin plus wortmannin treatment. A quantitative analysis of five different experiments was performed using Melanie software to compare the extent of phosphorylation of individual spots with the different treatments. These data are summarized in Tables I and II, with the corresponding spots indicated in Figs. 1 and 2. Insulin increased the phosphorylation of 18 different spots and decreased the phosphorylation of one row of phosphospots (C12). The insulin-dependent increase in phosphorylation among these different spots ranged in magnitude from 2-fold (C69, C95, H62, and H74) to >10-fold (C65, C79, H56, and H75) over basal. Some of the spots appeared to be phosphorylated under basal conditions (C2, C69, C95, H62, and H74). In fact for some of these there appeared to be a row of phosphospots that underwent a further leftward shift in response to insulin. This was most clearly observed for PKBβ (Fig. 4). However, in other cases we were unable to detect any significant phosphorylation under basal conditions (C65, C77, C79, H56, and H59). For these reasons it was difficult to precisely quantify the fold increase above basal in response to either insulin or PDGF, and so we have quantified each spot as a percentage of that observed in the presence of insulin.

Analysis of all the insulin-stimulated phosphoproteins in relation to their response to PDGF and wortmannin revealed that each of these spots fell into one of several different categories (see Fig. 5 for summary). Certain spots underwent a comparable increase in phosphorylation in response to both insulin and PDGF (C65, C77, C79, C95, H48, and H74). The majority of spots, however, were only phosphorylated in response to insulin (C2, C22, C49, C69, H38, H46, H56, H59, H60, H62, H72, H74, and H75). We did observe a slight increase in phosphorylation with PDGF for some of these proteins (C49, H46, H72, and H75) but this was not a reproducible phenomenon and the magnitude of this effect was less than that observed in response to insulin. Hence, these proteins were categorized as PDGF-insensitive, although it is conceivable that further analyses may reveal that they are PDGF responsive albeit to a lesser extent than insulin. Wortmannin abolished the insulin-stimulated phosphorylation of 16 spots but had no significant inhibitory effect on the insulin-induced phosphorylation of C22 and H48. However, the protein corresponding to H48 was also stimulated by PDGF and so does not represent an insulin-specific phosphoprotein. In addition, the

TABLE I

Characteristics of insulin-regulated cytosolic phosphoproteins

Statistical analysis was performed on insulin-stimulated cytosolic spots, as indicated in Fig. 1. Intensities are expressed as a percentage of the corresponding insulin-stimulated spot. The observed molecular mass and pI of insulin-stimulated phosphoproteins were calculated from identified landmark spots, by the Melanie II software. Spots which are PDGF-insensitive and wortmannin-sensitive (as determined by paired *t* tests) are shown in bold. MAPK, mitogen-activated protein kinase.

Spot no.	Molecular mass	pI	Relative value			n^a	Identity
			Basal	PDGF	Wortmannin/Insulin		
	kDa			*% of insulin*			
C2	**121**	**6.35–6.73**	**21.5 ± 7.2**[b]	**23.7 ± 9.5**	**25.4 ± 9.2**	**4**	**ACL**
C22	71	6.18	16.0 ± 13.7[b]	39.7 ± 26.5	65.3 ± 39.4[d]	4	
C49	**48**	**6.22**	**10.5 ± 7.8**[b]	**38.9 ± 20.4**	**16.7 ± 12.8**	**4**	
C65	44	6.01	3.9 ± 4.4[b]	71.4 ± 39.1[c]	0	4	MAPK
C69	**43**	**5.50**	**30.8 ± 12.7**[b]	**28.2 ± 18.4**	**13.8 ± 17.0**	**3**	
C77	41	6.27	9.2 ± 10.3[b]	63.0 ± 14.3[c]	2.6 ± 2.9	4	MAPK
C79	41	6.21	0[b]	127.2 ± 36.0[c]	0	4	
C95	35	6.17	42.0 ± 11.0[b]	126.3 ± 39.7[c]	39.2 ± 16.7	4	
C12	**95**	**6.95**	**171.9 ± 3.6**[b]	**190.1 ± 67.9**	**166.8 ± 43.6**	**4**	**EF2**

[a] n = number of data sets used for statistical analysis.
[b] $p < 0.05$ compared to insulin values (paired t test).
[c] $p < 0.05$ compared to basal values (paired t test).
[d] $p > 0.05$ compared to insulin values (paired t test).

TABLE II

Characteristics of insulin-regulated HSP phosphoproteins

Statistical analysis was performed on insulin-stimulated HSP spots, as indicated in Fig. 2. Intensities are expressed as a percentage of the corresponding insulin-stimulated spot. The observed molecular mass and pI of insulin-stimulated phosphoproteins were calculated from identified landmark spots, by the Melanie II software. Spots which are PDGF-insensitive and wortmannin-sensitive (as determined by paired *t* tests) are shown in bold.

Spot no.	Molecular mass	pI	Relative value			n^a
			Basal	PDGF	Wortmannin/Insulin	
	kDa			*% of insulin*		
H38	**61**	**6.16**	**9.2 ± 10.6**[b]	**19.9 ± 24.4**	**0**	**3**
H46	**56**	**6.15**	**20.6 ± 11.0**[b]	**53.6 ± 17.6**	**26.8 ± 16.5**	**3**
H48	49	4.86	24.3 ± 15.1[b]	86.7 ± 20.1[c]	73.9 ± 17.0[d]	5
H56	**48**	**6.22**	**1.5 ± 1.7**[b]	**13.0 ± 8.7**	**1.8 ± 2.0**	**4**
H59	**45**	**6.26**	**7.5 ± 8.4**[b]	**17.7 ± 15.5**	**15.7 ± 18.2**	**4**
H60	**43**	**6.34**	**15.8 ± 17.6**[b]	**12.3 ± 11.1**	**15.8 ± 18.3**	**4**
H62	**42**	**6.43**	**40.1 ± 19.6**[b]	**54.4 ± 2.3**	**23.5 ± 14.6**	**3**
H72	**40**	**6.18**	**10.0 ± 11.2**[b]	**50.3 ± 16.1**	**11.6 ± 11.7**	**4**
H74	39	6.27	37.2 ± 7.0[b]	79.0 ± 17.0[c]	41.7 ± 17.6	5
H75	**38**	**6.57**	**6.2 ± 4.4**[b]	**32.8 ± 13.7**	**7.0 ± 3.0**	**4**

[a] n = number of data sets used for statistical analysis.
[b] $p < 0.05$ compared to insulin values (paired t test).
[c] $p < 0.05$ compared to basal values (paired t test).
[d] $p > 0.05$ compared to insulin values (paired t test).

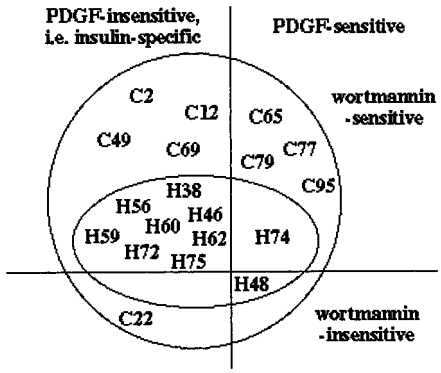

FIG. 5. **Insulin-specific phosphoproteins preferentially localize to the HSP fraction.** Insulin-regulated phosphoproteins (summarized in Tables I and II) were grouped by subcellular location (cytosol *versus* HSP), sensitivity to PDGF stimulation, and the effect of wortmannin on insulin-induced phosphorylation.

response to wortmannin for C22 was somewhat variable in that in three experiments wortmannin had no effect on insulin-stimulated C22 phosphorylation, whereas it caused complete inhibition in two other experiments.

Analysis of the subcellular distribution of insulin-regulated phosphoproteins suggested that insulin-specific (*i.e.* PDGF-insensitive) phosphoproteins preferentially localized to the HSP, with 62% found in this fraction (Fig. 5). On the other hand, only 30% of PDGF-sensitive phosphoproteins were in the HSP fraction (Fig. 5). The preferential localization of insulin-specific phosphoproteins in the HSP is consistent with the reported lack of PDGF-stimulated PI3K activity in this fraction (13, 14, 18) and further suggest that some insulin signaling pathways may be sequestered in a subcellular compartment, which fractionates in the HSP.

Identification of C2 as ATP-citrate Lyase—In an attempt to identify some of the insulin-specific phosphoproteins picked up in our screen, we scaled up the isolation procedure as described under "Experimental Procedures." Several of our candidate phosphospots were purified to Coomassie-stained bands, digested with trypsin, and subjected to liquid chromatography-MS. One of these spots contained sequences that correspond to a protein previously described to undergo insulin-stimulated phosphorylation. This protein, designated as C2 in our screen, was ACL (Fig. 6 and Table III), an enzyme which catalyzes the first step in fatty acid synthesis, the formation of acetyl-CoA (34, 35). Five differentially charged forms of phosphorylated ACL were consistently observed in the cytosol from insulin-stimulated adipocytes (Fig. 6*B*). A low level of ACL phosphorylation was observed in the basal state; however, the spots

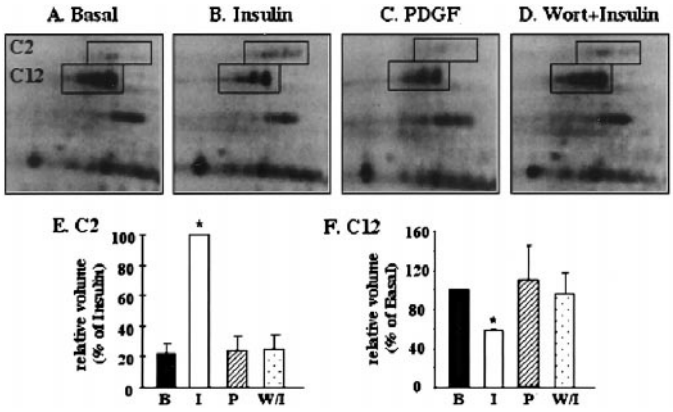

FIG. 6. **Insulin regulates the phosphorylation of C2 (ATP-citrate lyase) and C12 (elongation factor 2).** The basic, high molecular mass region of cytosol phosphorylation maps from a representative experiment is shown for basal (*A*), insulin-stimulated (*B*), PDGF-stimulated (*C*), and wortmannin-plus-insulin-treated (*D*) adipocytes. The rows of phosphospots corresponding to C2 and C12 are indicated. *E* and *F*, the phosphorylation of C2 and C12 was quantitated from four separate experiments and expressed as a percentage of the insulin-stimulated (*E*) or basal (*F*) value. *B*, basal; *I*, insulin-stimulated; *P*, PDGF-stimulated; *W/I*, wortmannin-plus-insulin-treated.

phosphorylated varied between the two most acidic spots (Fig. 6*A*, $n = 2$) and the three most basic spots (not shown, $n = 3$). Insulin caused a 5-fold increase in ACL phosphorylation, which was inhibited by wortmannin pretreatment (Table I and Fig. 6). The identification of this protein in our screen provides further validation for the integrity of the screen, because based on previous studies (34, 35) we would have expected this molecule to have been resolved using this type of approach.

Insulin Decreases the Phosphorylation of Elongation Factor 2—A row of constitutively phosphorylated spots that underwent insulin-dependent dephosphorylation (C12) was identified by liquid chromatography-MS as translation elongation factor 2 (EF2, Fig. 6, Table III). EF2 is a GTP-binding protein that mediates the translocation step in translation elongation and is completely inactivated when phosphorylated (reviewed in Ref. 36). It was recently reported that insulin decreases EF2 phosphorylation in Chinese hamster ovary cells overexpressing the insulin receptor (37) and in adipocytes (38). In the present study, we have also observed a significant insulin-dependent decrease in EF2 phosphorylation in 3T3-L1 adipocytes (Fig. 6). The magnitude of the decrease (2-fold) observed in our study is comparable to that reported previously (38). In contrast to that study, however, 3 distinct phosphospots were resolved by 2-DE (Fig. 6), consistent with the reported three phosphorylation sites in EF2 (39). Insulin-induced dephosphorylation was not specific for any charged isoform of EF2, and was prevented by wortmannin pretreatment (Fig. 6). PDGF had no significant effect on EF2 phosphorylation (Fig. 6).

DISCUSSION

The purpose of these studies was to test the hypothesis that insulin activates glucose metabolism by activating the PI3K/PKB pathway as well as another PI3K-independent pathway. Whereas overwhelming evidence has been presented to implicate a role for PI3K/PKB in this pathway, it has recently been suggested that activation of PI3K may not be sufficient to replicate the effects of insulin on glucose metabolism. Perhaps the most provocative study in favor of a PI3K-independent pathway was performed by Tsien and colleagues (19) who showed that a membrane-permeable PIP_3 analog had no effect on glucose transport in adipocytes *per se*. However, this compound was capable of suppressing the effects of a PI3K inhibitor, wortmannin, on insulin-stimulated glucose transport (19). Hence, this would support a role for PI3K and an additional PI3K-independent pathway in the regulation of glucose metabolism by insulin. In an effort to identify constituents of this so-called insulin-activated PI3K-independent pathway, we have used two-dimensional gel mapping of phosphoproteins in 3T3-L1 adipocytes. This screen relies on several major assumptions: (*a*) the alternate pathway involves, at some level, protein phosphorylation/dephosphorylation; (*b*) wortmannin does not inhibit the alternate pathway, which based on previous studies by Tsien and colleagues (19) seems likely; (*c*) that if such phosphoproteins do exist they will be present in sufficient abundance to be resolved by subcellular fractionation and 2-DE; and (*d*) PDGF will not activate this pathway because it activates PI3K, yet does not stimulate glucose uptake in adipocytes.

Using a subtraction-based analysis employing 2-DE, we find no evidence to support the existence of an insulin-stimulated PI3K-independent pathway involving protein phosphorylation in adipocytes. We detected at least 18 distinct spots that likely correspond to discrete proteins whose phosphorylation was increased by insulin. PDGF increased the phosphorylation of six of these proteins, whereas it had no significant effect on the remaining 12 spots (Fig. 5). Remarkably, wortmannin caused complete inhibition of the phosphorylation of 11 of these 12 insulin-specific phosphoproteins. Hence, in light of the above assumptions concerning the technique used here, these data provide compelling support in favor of the existence of an insulin-specific signaling pathway in adipocytes where almost all of the protoconstituents of this pathway are likely downstream of PI3K.

If there is no insulin-specific PI3K-independent pathway in adipocytes, this raises the important question as to how insulin, but not PDGF, activates a unique subset of downstream phosphoproteins when both growth factors appear to activate PI3K. One possibility that we (18) and others (13, 14) favor is that insulin activates PI3K in a unique location within the cell and that this may allow the enzyme to access a unique repertoire of downstream proteins. We have gathered evidence in favor of this hypothesis in the present study because we observed that most of the insulin-specific phosphoproteins were localized to the same subcellular fraction as the insulin-dependent PI3K activity (Fig. 5). Most notably the PDGF-stimulated PI3K activity is found in a separate fraction (13, 14, 18). Another possibility that is perhaps not mutually exclusive to that described above is that insulin and PDGF may activate unique PI3K isoforms. This would not be surprising because we have recently observed that insulin preferentially activates the PKBβ isoform in adipocytes (8). Yet another possibility revolves around the fact that PI3K possesses both lipid and protein kinase activities. It has recently been reported that the protein kinase activity of PI3K may selectively regulate mitogen-activated protein kinase activity, whereas its lipid kinase activity may selectively activate PKB (40). Wortmannin binds to the ATP binding site in PI3K and so inhibits both the protein and lipid kinase activities. Hence this would potentially explain why in the present studies we observe inhibition of almost all insulin-specific phosphoproteins by wortmannin. It remains possible that the protein kinase activity of PI3K mediates the so-called alternate pathway because PIP_3 analogs only partially rescued the wortmannin block of insulin-stimulated glucose uptake in adipocytes (19). Recent experiments using plasma membrane recruitment of green fluorescent protein-tagged ADP ribosylation factor nucleotide-binding site opener (ARNO) as an assay for PIP_3 production have failed to find a significant effect of PDGF in adipocytes (41). This suggests that although PI3K is recruited to the PDGF receptor in

TABLE III

Analysis of C2 and C12 by liquid chromatography-electrospray ionization-ion trap mass spectrometry

Spots C2 and C12 were purified from insulin-stimulated 3T3-L1 adipocytes, digested with trypsin, and then analysed by liquid chromatography mass spectrometry as described under "Experimental Procedures."

Spot no.	Identification	Swissprot accession no.	Peptide no.	Sequence	Position in protein
C2	ATP-citrate lyase	P16638	1	NFLIEPFVPHSQAEEFY	104–120
			2	IGNTGGMLDNILASK	645–659
			3	SFDELGEIIQSVYEDLVAK	788–806
			4	FGGALDAAAK	933–943
C12	Elongation factor 2	P05197	1	VNFTVDQIR	2–10
			2	DGSGFLINLIDSPGHVDFSSEVTAALR	93–120
			3	CELLYEGPPDDEAAMGIK	369–386
			4	VFSGVVSTGLK	416–426
			5	EDLYLKPIQR	440–449
			6	YVEPIEDVPCGNIVGLVGVDQFLVK	457–481
			7	TGTITTFEHAHNMR	482–495
			8	GVQYLNEIK	668–676
			9	GHVFEESQVAGTPMFVVK	768–785

response to PDGF in these cells (13, 14, 18), for some reason the accumulation of PIP_3 is blunted. Consistent with this, we have recently reported that PDGF does not induce the phosphorylation or membrane translocation of PKBβ in adipocytes (8). This failure to stimulate PIP_3 levels may be because of either a block in production, possibly because the PDGF receptor does not have access to phosphatidylinositol 4,5-bisphosphate, or to an increased degradation of PIP_3. In the case of the latter, it is conceivable that the PDGF receptor binds a phospholipid phosphatase that selectively hydrolyses PIP_3 produced in response to PDGF, but not other ligands such as insulin. Despite the inability of PDGF to increase PIP_3 levels in adipocytes, it seems clear from the present studies that PDGF stimulates the protein kinase activity of PI3K, because we observed a marked increase in MAP kinase activity in response to both insulin and PDGF, and this was inhibited by wortmannin (Table I). Thus, it seems plausible that both the lipid and protein kinase activities of PI3K augment separate downstream signaling pathways in adipocytes, and both may be required to activate glucose metabolism.

The present studies have clearly resolved a number of proteins that are insulin-specific and wortmannin-sensitive and thus constitute excellent candidates for downstream molecules in insulin action. We have attempted to characterize many of these proteins using liquid chromatography-MS; however, with the exception of two proteins (Table III) the success of these studies has been limited. This is due in part to inadequate resolution of the preparative 2-DE system because many of the spots identified contain >5–9 separate polypeptides (data not shown). Thus, in order to extend these studies it may be necessary to incorporate additional purification steps prior to 2-DE. It is also possible that many of the proteins we are working with are very low abundance necessitating a much larger scale than has been currently employed. Nevertheless in view of the potential importance of some of the molecules identified here, additional experiments are probably warranted. The identification of ATP-citrate lyase as one of our candidate proteins in part validated the use of this technique because this protein is known to be phosphorylated by insulin in a wortmannin-sensitive manner. This result also indicates that this approach will enable us to achieve nonselective identification of both signaling proteins such as MAP kinase and PKB (Figs. 3 and 4) as well as metabolic machinery (Fig. 6). Furthermore, this approach can be used to detect both increases and decreases in protein phosphorylation both of which are affected by insulin. The only significant protein dephosphorylation event we were able to detect corresponded to the other protein we were able to positively identify by MS and that was eucaryotic elongation factor 2 (Table III and Fig. 6). This protein is a key regulatory determinant of mRNA translation, and this process is known to be influenced by insulin stimulation. To complement the recent studies reporting insulin-dependent EF2 dephosphorylation, our data further suggest that dephosphorylation of EF2 is wortmannin-sensitive and PDGF-insensitive in adipocytes.

In summary, we have identified a number of proteins that are phosphorylated in an insulin-specific and wortmannin-sensitive manner. The absence of insulin-specific wortmannin-insensitive proteins calls into question the existence of a PI3K-independent pathway in adipocytes. Recent studies also suggest that PI3K is involved in insulin regulation of metabolism in the liver (42, 43). Interestingly, in hepatocytes insulin also stimulates PI3K activity in a fraction similar to the high speed pellet fraction of adipocytes (43). Indeed many of the insulin-specific phosphoproteins we have mapped in the current study are enriched in the HSP fraction that also contains the insulin responsive IRS proteins (13, 14, 18, 43), adding further support to the concept that localization of signaling molecules may play an important role in their specific function.

Acknowledgments—We thank Morris Birnbaum (HHMI, Pennsylvania, PA), Michael Felder (University of South Carolina, Columbia, SC), David Klein (National Institutes of Health, Bethesda, MD) and George Janssen (Leiden University, Leiden, The Netherlands) for providing the antibodies used during the course of these studies. We also thank Teresa Munchow, Hong Ji, and Ning-Xia Fang for technical assistance and members of the James laboratory for helpful discussions.

REFERENCES

1. James, D. E., and Piper, R. C. (1994) *J. Cell Biol.* **126,** 1123–1126
2. DeFronzo, R. A., Bonadonna, R. C., and Ferrannini, E. (1992) *Diabetes Care* **15,** 318–368
3. Clarke, J. F., Young, P. W., Yonezawa, K., Kasuga, M., and Holman, G. D. (1994) *Biochem. J.* **300,** 631–635
4. Cheatham, B., Vlahos, C. J., Cheatham, L., Wang, L., Blenis, J., and Kahn, C. R. (1994) *Mol. Cell. Biol.* **14,** 4902–4911
5. Sharma, P. M., Egawa, K., Huang, Y., Martin, J. L., Huvar, I., Boss, G. R., and Olefsky, J. M. (1998) *J. Biol. Chem.* **273,** 18528–18537
6. Kotani, K., Carozzi, A. J., Sakaue, H., Hara, K., Robinson, L. J., Clark, S. F., Yonezawa, K., James, D. E., and Kasuga, M. (1995) *Biochem. Biophys. Res. Commun.* **209,** 343–348
7. Cong, L. N., Chen, H., Li, Y., Zhou, L., McGibbon, M. A., Taylor, S. I., and Quon, M. J. (1997) *Mol. Endocrinol.* **11,** 1881–1890
8. Hill, M. M., Clark, S. F., Tucker, D. F., Birnbaum, M. J., James, D. E., and Macaulay, S. L. (1999) *Mol. Cell. Biol.* **19,** 6661–6671
9. Martin, S. S., Haruta, T., Morris, A. J., Klippel, A., Williams, L. T., and Olefsky, J. M. (1996) *J. Biol. Chem.* **271,** 17605–17608
10. Kohn, A. D., Summers, S. A., Birnbaum, M. J., and Roth, R. A. (1996) *J. Biol. Chem.* **271,** 31372–31378
11. Nystrom, F. H., and Quon, M. J. (1999) *Cell. Signalling* **11,** 563–574
12. Isakoff, S. J., Taha, C., Rose, E., Marcusohn, J., Klip, A., and Skolnik, E. Y. (1995) *Proc. Natl. Acad. Sci. U. S. A.* **92,** 10247–10251
13. Nave, B. T., Haigh, R. J., Hayward, A. C., Siddle, K., and Shepherd, P. R. (1996) *Biochem. J.* **318,** 55–60
14. Ricort, J. M., Tanti, J. F., Van Obberghen, E., and Le Marchand-Brustel, Y. (1996) *Eur. J. Biochem.* **239,** 17–22
15. Huppertz, C., Schwartz, C., Becker, W., Horn, F., Heinrich, P. C., and Joost, H. G. (1996) *Diabetologia* **39,** 1432–1439

16. Wiese, R. J., Mastick, C. C., Lazar, D. F., and Saltiel, A. R. (1995) *J. Biol. Chem.* **270,** 3442–3446
17. Quon, M. J., Chen, H., Lin, C. H., Zhou, L., Ing, B. L., Zarnowski, M. J., Klinghoffer, R., Kazlauskas, A., Cushman, S. W., and Taylor, S. I. (1996) *Biochem. Biophys. Res. Commun.* **226,** 587–594
18. Clark, S. F., Martin, S., Carozzi, A. J., Hill, M. M., and James, D. E. (1998) *J. Cell Biol.* **140,** 1211–1225
19. Jiang, T., Sweeney, G., Rudolf, M. T., Klip, A., Traynor-Kaplan, A., and Tsien, R. Y. (1998) *J. Biol. Chem.* **273,** 11017–11024
20. Robinson, L. J., Razzack, Z. F., Lawrence, J. C. Jr., and James, D. E. (1993) *J. Biol. Chem.* **268,** 26422–26427
21. Hill, M. M., Clark, S. F., and James, D. E. (1997) *Electrophoresis* **18,** 2629–2637
22. Towbin, H., Staehelin, T., and Gordon, J. (1979) *Proc. Natl. Acad. Sci. U. S. A.* **76,** 4350–4354
23. Arand, M., Friedberg, T., and Oesch, F. (1994) in *Cell Biology: A Laboratory Handbook* (Celis, J. E., ed) Vol. 3, pp. 276–278, Academic Press, London
24. Gevaert, K., Verschelde, J. L., Puype, M., Van Damme, J., Goethals, M., De Boeck, S., and Vandekerckhove, J. (1996) *Electrophoresis* **17,** 918–924
25. Moritz, R. L., Eddes, J. S., Reid, G. E., and Simpson, R. J. (1996) *Electrophoresis* **17,** 907–917
26. Moritz, R. L., Reid, G. E., Ward, L. D., and Simpson, R. J. (1994) *Methods Enzymol.* **6,** 213–226
27. Eng, J. K., McCormack, A. L., and Yates, J. R., III (1994) *J. Am. Soc. Mass Spectrom.* **5,** 976–989
28. Lawrence, J. R., Jr. (1992) *Annu. Rev. Physiol.* **54,** 177–193
29. Avruch, J., Leone, G. R., and Martin, D. B. (1976) *J. Biol. Chem.* **251,** 1505–1510
30. Avruch, J., Leone, G. R., and Martin, D. B. (1976) *J. Biol. Chem.* **251,** 1511–1515
31. Guy, G. R., Philip, R., and Tan, Y. H. (1994) *Electrophoresis* **15,** 417–440
32. Levenson, R. M., and Blackshear, P. J. (1989) *J. Biol. Chem.* **264,** 19984–19993
33. Kohn, A. D., Kovacina, K. S., and Roth, R. A. (1995) *EMBO J.* **14,** 4288–4295
34. Ramakrishna, S., and Benjamin, W. B. (1979) *J. Biol. Chem.* **254,** 9232–9236
35. Alexander, M. C., Kowaloff, E. M., Witters, L. A., Dennihy, D. T., and Avruch, J. (1979) *J. Biol. Chem.* **254,** 8052–8056
36. Proud, C. G., and Denton, R. M. (1997) *Biochem. J.* **328,** 329–341
37. Redpath, N. T., Foulstone, E. J., and Proud, C. G. (1996) *EMBO J.* **15,** 2291–2297
38. Diggle, T. A., Redpath, N. T., Heesom, K. J., and Denton, R. M. (1998) *Biochem. J.* **336,** 525–529
39. Ovchinnikov, L. P., Motuz, L. P., Natapov, P. G., Averbuch, L. J., Wettenhall, R. E., Szyszka, R., Kramer, G., and Hardesty, B. (1990) *FEBS Lett.* **275,** 209–212
40. Bondeva, T., Pirola, L., Bulgarelli-Leva, G., Rubio, I., Wetzker, R., and Wymann, M. P. (1998) *Science* **282,** 293–296
41. Oatey, P. B., Venkateswarlu, K., Williams, A. G., Fletcher, L. M., Foulstone, E. J., Cullen, P. J., and Tavare, J. M. (1999) *Biochem. J.* **344,** 511–518
42. Carlsen, J., Christiansen, K., Grunnet, N., and Vinten, J. (1999) *Cell. Signalling* **11,** 713–717
43. Phung, T. L., Roncone, A., de Mesy Jensen, K. L., Sparks, C. E., and Sparks, J. D. (1997) *J. Biol. Chem.* **272,** 30693–30702

Differential Protein Phosphorylation in 3T3-L1 Adipocytes in Response to Insulin *Versus* Platelet-derived Growth Factor: NO EVIDENCE FOR A PHOSPHATIDYLINOSITIDE 3-KINASE-INDEPENDENT PATHWAY IN INSULIN SIGNALING

Michelle M. Hill, Lisa M. Connolly, Richard J. Simpson and David E. James

J. Biol. Chem. 2000, 275:24313-24320.
doi: 10.1074/jbc.M001823200 originally published online May 8, 2000
